Generation of initial fields for channel flow investigation

Markus Uhlmann
Potsdam Institut für Klimafolgenforschung, D-14412 Potsdam
uhlmann@pik-potsdam.de

(Mai 2000)

In the framework of the DFG-funded research project KL 611/10, detailed time-dependent information of the flow fields in two distinct geometric configurations (homogeneous, isotropic flow; plane channel flow) is needed for the purpose of analyzing the behavior of small-scale instabilities and their influence upon the turbulent energy cascade. Here we describe the method of generating those fields via direct numerical simulation (DNS) in the latter case of plane channel flow.

For our pseudo-spectral Fourier-Chebyshev computations, the physical and numerical parameters are chosen with reference to the work of Moser, Kim & Mansour (1999) (additional data is available in (AGARD Advisory Report No. 345 1997, case PCH10)) who investigated channel flow at friction-velocity-based Reynolds numbers of $Re_\tau = u_\tau\, h/\nu = \{395, 590\}$. These values were adopted for our present study. The respective values of the alternative Reynolds numbers based upon the centerline velocity U_0 and the bulk velocity $U_b = \int_0^{2h} U(y)dy/(2h)$ can be found in table 1. We selected the size of our computational box ($L_x \times 2h \times L_z$) as well as the numerical resolution identical to the values of Moser *et al.* (1999). Note that for the current choice, very large structures are expected to be constrained by the numerical periodicity requirement (cf. Jiménez (1998, 2000)). However, this fact only presents an inconvenience if one regards the simulation as a model for a flow in an infinite spanwise/streamwise domain (cf. (AGARD Advisory Report No. 345 1997, p.119)). Since the specific interest of our study is focussed upon the ultraviolet end of the turbulent spectrum, we consider the current box size (more than 10 minimal flow units in each direction, Jiménez & Moin (1991)) as adequate. The case with the lowest Reynolds number ($Re_\tau = 180$) indicated in table 1 served us in the process of generating initial turbulent fields for the two simulation runs by providing realistic fluctuations.

Our numerical algorithm is essentially equivalent to the method of Kim, Moin & Moser (1987) where the interested reader can find more details. Let us simply recall that a toroidal/poloidal decomposition is used where evolution equations are solved for the wall-normal vorticity $\omega_y = u_{,z} - w_{,x}$ and the laplacian of the wall-normal velocity $\varphi = \nabla^2(v)$. The mean flow equations for the streamwise and spanwise velocity are solved separately.

The actual initial fields were generated from two different components.

1) The mean flow profile $U(y)$ (which corresponds to the constant mode $\hat{u}(k_x = 0, y, k_z = 0)$ of the Fourier-transformed velocity field) was imposed directly from the statistical data of Moser *et al.* (1999), viz.:

$$U(y, t_0) = \overline{U}(y)_{Moser\,et\,al.} / \overline{U}(y = h)_{Moser\,et\,al.} \quad , \tag{0.1}$$

where the overbar indicates time-averaging. Our code is designed in a way that drives the constant mode dynamics such as to ensure a time-constant mass flow, $U_b = cst$. By choosing $U(y = h, t_0) = 1$ we can directly impose $1/Re_0$ from table 1 as the viscosity.

2) The fluctuations of ω_y, φ are taken from an instantaneous (fully-developed) field of

Re_τ	Re_0	Re_b	L_x	L_z	$N_x \times N_y \times N_z$	Δ_x^+	Δ_z^+	Δ_y^+
180	3250	2925	$3\pi h$	πh	192× 97×128	8.8	4.4	5.9
395	7881	6876	$2\pi h$	πh	256×193×256	10.0	6.5	6.5
590	12486	10972	$2\pi h$	πh	384×257×384	9.7	4.8	7.2

TABLE 1. Parameters of the three plane channel flow simulations: friction-velocity-based, centerline-velocity-based and bulk-velocity-based Reynolds number; box size; number of modes (before de-aliasing); equivalent grid size (note that Δ_y^+ corresponds to the maximum vertical grid size near the centerline).

the low-Reynolds case at $Re_\tau = 180$. First, data in Fourier space is copied into the lower wavenumbers and then the remaining coefficients are filled up with zeroes, viz.

$$\hat{\omega}_y(k_x, k_y, k_z, t_0) = \begin{cases} \hat{\omega}_y(k_x, k_y, k_z, t_1)_{Re_\tau=180} & \text{if } k_x \leq 192 \cup k_y \leq 97 \cup k_z \leq 128 \\ 0 + i \cdot 0 & \text{else} \end{cases}, \tag{0.2}$$

and similarly for φ.

Therefore, we expect an initial transient phase due to the following four effects:

(i) sudden decrease of molecular viscosity;

(ii) addition of numerical degrees of freedom;

(iii) change in box-size (L_x : $3\pi h \rightarrow 2\pi h$);

(iv) mismatch between constant mode profile and the field of fluctuations.

Figure 1 shows that in both cases the plane-averaged skin friction rapidly decreases before returning to its initial value by $t\,U_0/h \approx 35 \ldots 40$. The high-Re case recovers more rapidly, which indicates that the effect might scale in wall units rather than in outer flow time units. The transient behavior shows that the initial low-Re fluctuations cannot sustain the near-wall gradient of $U(y)$ taken from the high-Re statistics. The observed transient time is related to the adaptation of the near-wall cycle to the new conditions (i)-(iv).

After discarding the initial transient phase we started accumulating first and second order one-point statistics in order to verify that our sequence corresponds to a fully-developed state. Figure 2 shows the time-averaged mean velocity profile and figure 3 several components of the Reynolds stress tensor for the high-Re case. The agreement with data from Moser *et al.* (1999) is satisfactorily considering the relatively short "useful" integration interval of $69.5h/U_0$. Figure 4 confirms the state of the convergence of our statistics by demonstrating that the sum of the viscous and turbulent shear stresses varies linearly across the channel.

The MPI-based computation of the full time-sequence in the high-Re case ($\Delta t U_0/h = 98.27$) has taken 84h of individual CPU time on 128 processors of the CRAY T3E LC384 machine at ZIB, Berlin.

The code for the present simulation was kindly provided by J. Jiménez and A. Pinelli of ETSI Aeronauticos, Universidad Politécnica, Madrid. The computational resources of ZIB, Berlin, are gratefully acknowledged.

REFERENCES

AGARD Advisory Report No. 345 1997 A selection of test cases for the validation of large-eddy simulations of turbulent flows. available at ftp://138.4.75.138/.

JIMÉNEZ, J. 1998 The largest scales of turbulent wall flows. *CTR Res. Briefs* pp. 137–154.

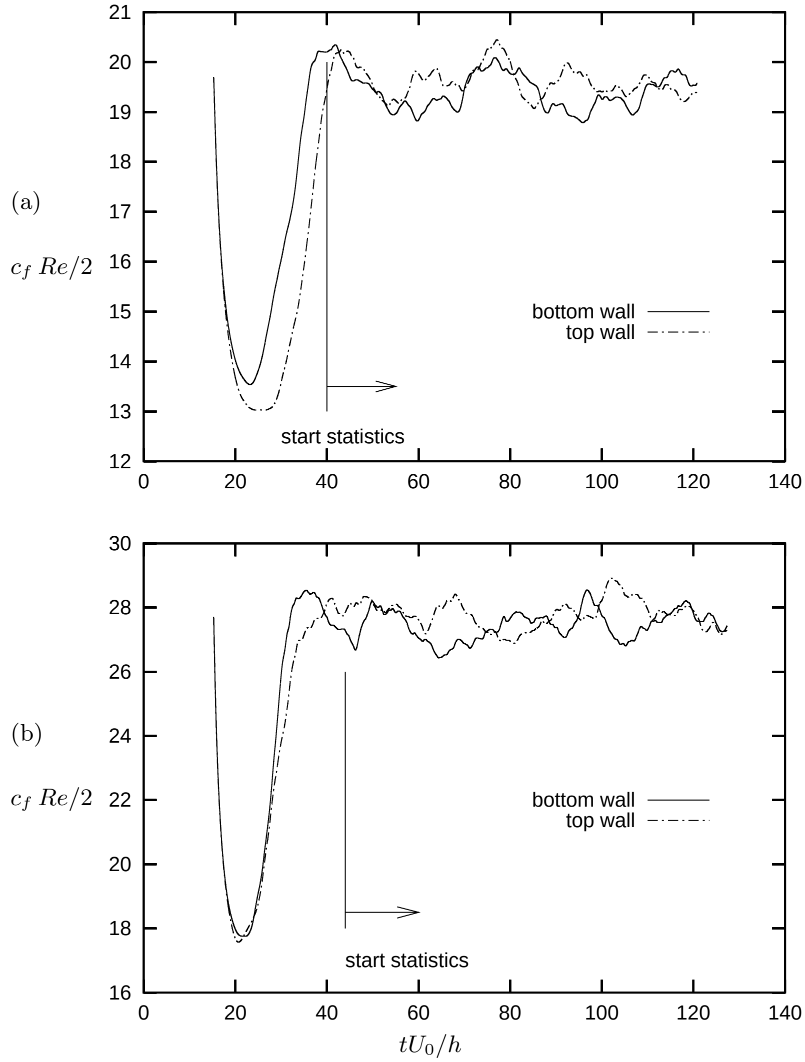

FIGURE 1. Temporal evolution of the plane-averaged skin friction c_f during the initial sequence of the plane channel flow simulation. The strong initial transient is due to the generation procedure of the initial field as described in the text. (a) $Re_\tau = 395$; (b) $Re_\tau = 590$.

JIMÉNEZ, J. 2000 Some open computational problems in wall-bounded turbulence. In *Advances in Turbulence VIII* (ed. C. D. et al.), pp. 637–646. Barcelona, Spain.

JIMÉNEZ, J. & MOIN, P. 1991 The minimal flow unit in near-wall turbulence. *J. Fluid Mech.* **225**, 213–240.

KIM, J., MOIN, P. & MOSER, R. 1987 Turbulence statistics in a fully developed channel flow at low Reynolds number. *J. Fluid Mech.* **177**, 133–166.

MOSER, R., KIM, J. & MANSOUR, N. 1999 Direct numerical simulation of turbulent channel flow up to $Re_\tau = 590$. *Phys. Fluids* **11** (4), 943–945.

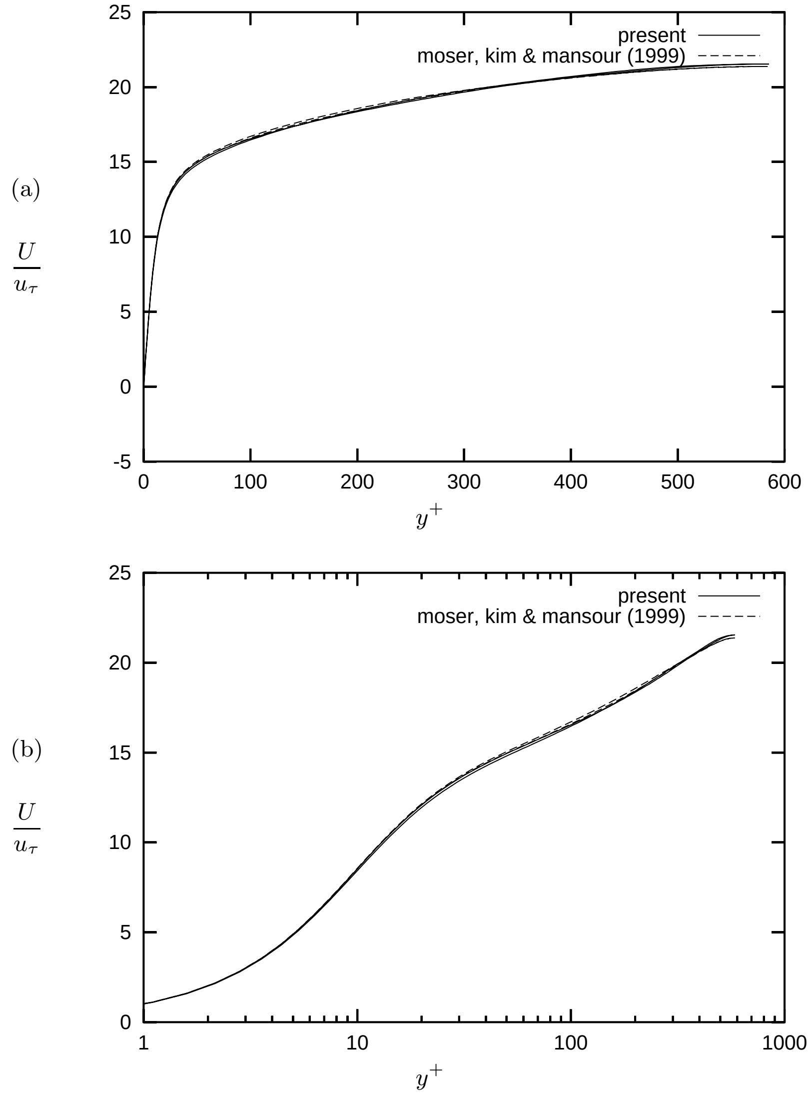

FIGURE 2. Mean velocity profile of the $Re_\tau = 590$ case. Lines for the bottom and the top half of the channel are superposed such as to provide an estimate of the statistical uncertainty. (a) lin-lin plot; (b) log-lin plot.

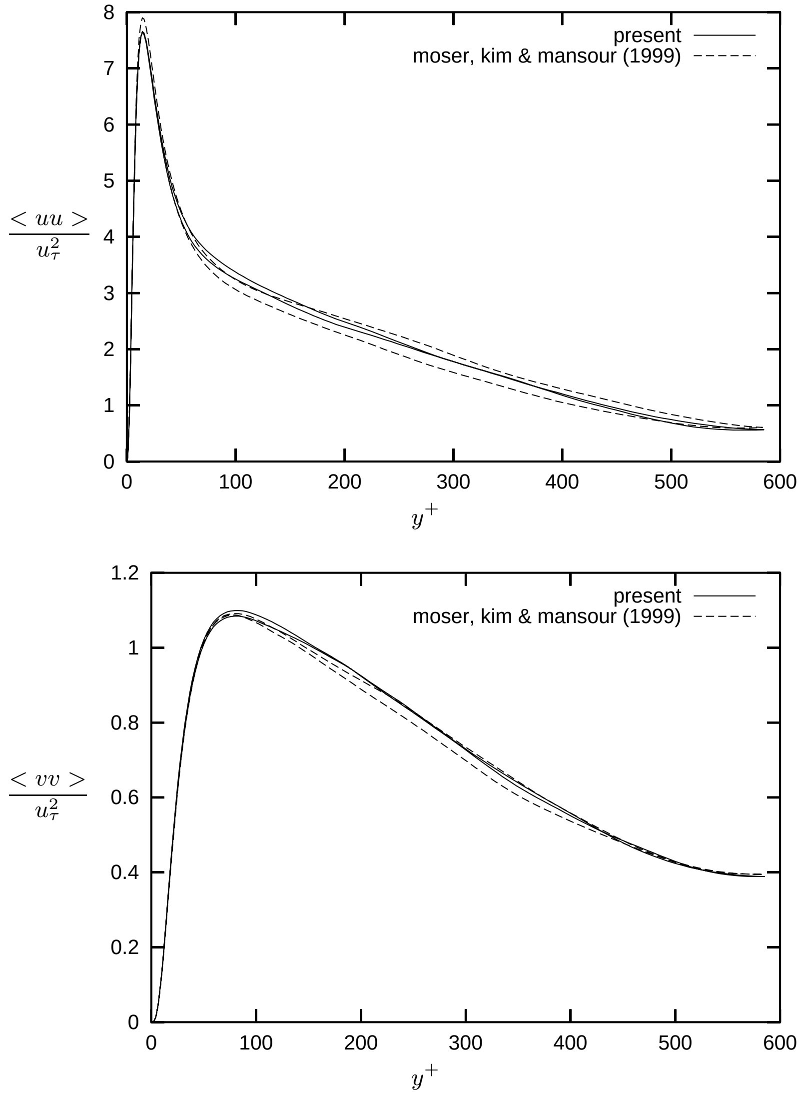

FIGURE 3. Wall-normal profile of various components of the Reynolds stress tensor of the $Re_\tau = 590$ case. Lines for the bottom and the top half of the channel are superposed such as to provide an estimate of the statistical uncertainty.

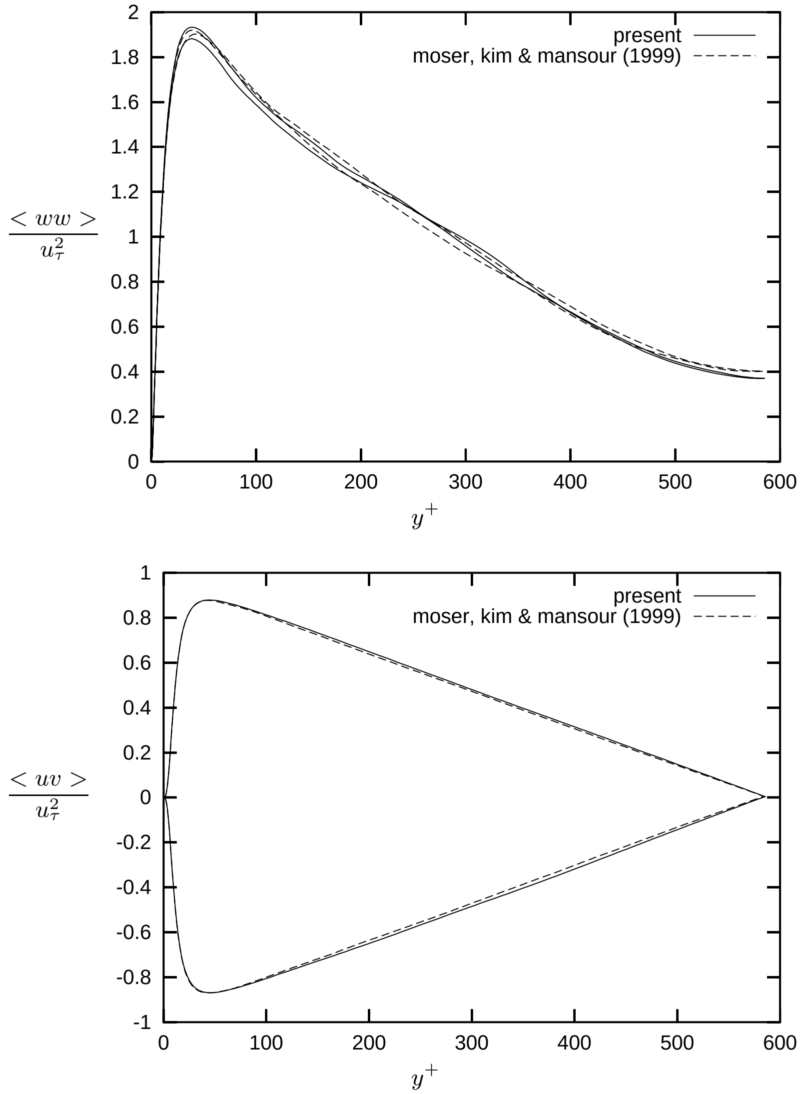

FIGURE 3. *(continued)*

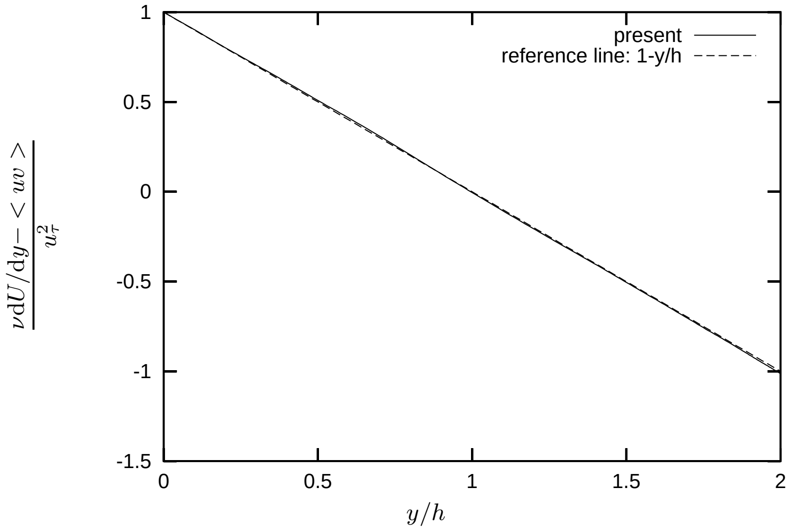

FIGURE 4. Wall-normal profile of the total shear stress of the $Re_\tau = 590$ case.